Supporting Information

Mitchell et al. 10.1073/pnas.1121051109

SI Text

Model Equations and Description. The model is described below, with all parameters defined in detail in Table S1. For consistency with the earlier deterministic analysis, parameters in the deterministic models that were yearly rates are kept as yearly rates here but are converted into probabilities within the model equations and then converted into daily probabilities by dividing by *dpy* (days per year).

The infection process. Each individual in the models has an underlying maximum yearly contact rate Λ_m, drawn from a gamma distribution that has a mean equal to the average population maximum yearly contact rate Λ_{pmax} ($\Lambda_m \sim \text{Gamma}(k_1, \Lambda_{\text{pmax}}/k_1)$, where k_1 is the shape parameter of the gamma distribution). Λ_m is selected in this way at the start of the simulation (when $a = 0$) and is reselected in the same way with a yearly probability ϕ, so at each (daily) time step there is a probability ϕ/dpy that an individual's underlying maximum contact rate will be recalculated (where $dpy = 365$). If ϕ is 0, this assumes perfect predisposition, with individuals maintaining the same level of exposure for life. Positive values of ϕ represent individuals making sudden changes in their contact rate, which might happen if they move house or change school or occupation. Here, ϕ is based upon rates at which people reported moving house in a Zimbabwean study population. In this population, a negative correlation was found between infection intensity and distance lived from the nearest water-contact site in young children, suggesting that location of residence is a strong determinant of exposure level (see *Estimating* ϕ).

In line with field observations from Zimbabwe (1), an individual's contact rate is assumed to increase linearly with age up to age a_c and then remain constant at a yearly rate Λ_m:

$$\Lambda(a) = \begin{cases} \Lambda_m \frac{a}{a_c} & \text{if } a < a_c, \\ \Lambda_m & \text{if } a \geq a_c. \end{cases} \quad \text{[S1]}$$

On each day, the number of contacts, r, that an individual makes is drawn from a Poisson distribution with mean $\Lambda(a)/dpy$ ($r \sim \text{Pois}(\Lambda(a)/dpy)$). In line with earlier analyses, it is assumed that, on average, an individual acquires one schistosome cercaria per contact. To incorporate aggregation in cercarial infection, it is assumed that an individual acquires d cercariae with a probability $1/d$ per contact. t_q is the number of cercariae acquired on the qth contact ($q = 1, \ldots, r$) on each day such that

$$t_q = \begin{cases} d & \text{if } s < 1/d, \text{where } s \sim U(0,1) \\ 0 & \text{otherwise.} \end{cases} \quad \text{[S2]}$$

The total number of cercariae, b, acquired during a single day is therefore given by $b = \sum_{q=1}^{r} t_q$. New cercariae may be killed upon entry into the host by an anti-reinfection antibody response. It is assumed that cercariae are killed as a decreasing exponential function of protective antibody level (A_2), such that the probability of a cercaria surviving is $e^{-\theta A_2(a-1)}$. The number of surviving cercariae acquired on a given day, f, is binomially distributed, $f \sim \text{Binom}(b, e^{-\theta A_2(a-1)})$. The schistosomulum stage is not explicitly represented here; in reality, the larval stages take about 4–6 wk to reach maturity (becoming adult, egg-laying worms), but this is a relatively short period in comparison with the simulation time for these models (6–34 y) and is not included.

Live worms are modeled passing through nine compartments ($n = 9$) to give approximately Gaussian distributed worm survival. Newly acquired worms (f) enter the first worm compartment ($i = 1$). The rate at which a worm moves from compartment i to compartment $i + 1$ is $n\mu$ per year where $1/\mu$ is the average worm life span in years. Therefore the daily probability of a worm moving from compartment i to compartment $i + 1$ is $1 - e^{-n\mu/dpy}$. If compartment i contains $P_i(a-1)$ worms at age $a - 1$ the number of worms leaving it at age a, m_i, is binomially distributed ($m_i \text{Binom}(P_i(a-1), 1 - e^{-n\mu/dpy})$). Therefore the number of worms in compartment i at age a is given by

$$P_i(a) = \begin{cases} P_i(a-1) + f - m_i & \text{for } i = 1, \\ P_i(a-1) + m_{i-1} - m_i & \text{for } 1 < i \leq n. \end{cases} \quad \text{[S3]}$$

Worms die as they leave the final (nth) compartment (m_n gives the number of worms dying). The number of eggs stimulating an immune response (E) is assumed to be proportional to current worm burden, implying that immune stimulation is primarily by very recently laid eggs, potentially through antigens they secrete. E is reduced by anti-fecundity antibody. An anti-fecundity response is assumed to reduce E deterministically via a decreasing exponential function of antibody level, with relative strength η, $E(a) = \sum_{i=1}^{n} P_i(a) e^{-\eta A_2(a-1)}$, because the number of eggs stimulating the immune response is related to current worm burden.

Mean egg output (analogous to egg counts measured in urine) is calculated on a single day for each individual (sampling day), as the arithmetic mean of three separate "samples" (u_y for $y = 1, 2, 3$). Each sample is drawn from a negative binomial distribution (implemented as a Poisson distribution with a gamma-distributed mean), with mean $\varepsilon E(a)$ (where ε is the mean number of eggs output in 10 mL urine per worm per day) and aggregation parameter k_E. Mean egg output $= \sum_{y=1}^{3} u_y$, where $u \sim \text{Pois}(\text{Gamma}(k_E, \varepsilon E(a)/k_E))$.

The aggregation parameter for egg output (k_E) is taken from values calculated for *S. mansoni* (2).

Antibody responses. Two antibody responses (A_1 and A_2) are modeled as separate populations of plasma cells. It is assumed that antibody levels are directly proportional to the number of plasma cells at a given time. Plasma cell population dynamics are modeled deterministically. Each antibody response (the jth antibody response (where $j = 1, 2$)) has a single life stage (S_j) as its principal source of antigen, either cercariae, live worms, dying worms or eggs (within the host). The level of antigen (G_j) stimulating the jth antibody response at age a is calculated as follows:

$$G_j(a) = \begin{cases} b & \text{for } S_j = \text{cercarial antigen,} \\ \left(\sum_{i=1}^{n} P_i(a)\right)/dpy & \text{for } S_j = \text{live adult worm antigen,} \\ m_n & \text{for } S_j = \text{dying adult worm antigen,} \\ E(a)/dpy & \text{for } S_j = \text{internal egg antigen.} \end{cases} \quad \text{[S4]}$$

Levels of live worms and internal eggs are divided by the number of days per year (dpy) to give a direct comparison with the deterministic model output (3).

Two separate types of models are considered: those with cross-regulation of the nonprotective antibody response, and those with an antigen threshold for the protective antibody response. These are described in turn below.

The cross-regulation included in the model is a representation of the antagonism between different cytokine responses, which influence the nature and magnitude of the antibody response.

Each plasma cell population (A_j) expands at a rate proportional to the level of antigen stimulating that response (G_j), multiplied by a constant, κ_j. In models with cross-regulation, this rate of growth is down-regulated for the nonprotective antibody response, A_1, via a decreasing exponential function of the level of antigen stimulating the protective antibody response (G_2), with relative strength ρ. There is no cross-regulation of the protective antibody response in these models. Each plasma cell population decays with a yearly per cell rate γ_j, giving a daily cell loss of $1 - e^{-\gamma_j/dpy}$.

$$A_1(a) = A_1(a-1) + \kappa_1 G_1(a) e^{-\rho G_2(a)} - A_1(a-1)(1 - e^{-\gamma_1/dpy}) \quad \textbf{[S5]}$$

$$A_2(a) = A_2(a-1) + \kappa_2 G_2(a) - A_2(a-1)(1 - e^{-\gamma_2/dpy}), \quad \text{where } \gamma_1 \geq \gamma_2. \quad \textbf{[S6]}$$

In the threshold models, the requirement for a threshold level of cumulative antigen exposure represents the activation, proliferation, differentiation and survival of the T cell response, which is driven by accumulated exposure to antigen (4, 5), and in turn helps to generate and maintain the B cell response.

For models with an antigen threshold, a cumulative tally of exposure to antigen is kept (Eq. **S7**). The nonprotective plasma cell compartment (A_1) is unaffected by the threshold and grows at a rate proportional to the level of its antigen, G_1 (Eq. **S8**). The protective antibody response (A_2) is only made if the antigen cumulative exposure exceeds a threshold level, T (Eq. **S9** . Once this antigen threshold has been exceeded, the protective plasma cell compartment (A_2) grows at a rate proportional to the level of relevant antigen present (G_2), in the same way as in the cross-regulation model. Both plasma cell populations decay with a yearly per cell rate γ_j, as before.

$$C(a) = C(a-1) + \beta G_2(a) \quad \textbf{[S7]}$$

$$A_1(a) = A_1(a-1) + \kappa_1 G_1(a) - A_1(a-1)(1 - e^{-\gamma_1/dpy}) \quad \textbf{[S8]}$$

$$A_2(a) = \begin{cases} A_2(a-1) - A_2(a-1)(1 - e^{-\gamma_2/dpy}) & \text{if } C(a) < T, \\ A_2(a-1) + \kappa_2 G_2(a) - A_2(a-1)(1 - e^{-\gamma_2/dpy}) & \text{if } C(a) \geq T. \end{cases} \quad \textbf{[S9]}$$

Including treatment. The impact of treatment is assessed in the model by introducing treatment on a single day (the day after sampling) for all individuals aged 6–15 years old. The effects of treatment are assumed to be (i) a decline in worm burden, (ii) a boost to the level of dying worm antigen (proportional to the number of worms killed by treatment), and (iii) a reduction in transmission after treatment, modeled as a reduction in the probability of infection per contact on all subsequent days. The simulation is continued for a further 36 wk after treatment, with egg output and antibody levels recorded at 12, 18, 24, 30, and 36 wk post-treatment for individuals aged 6–15 years old.

With a given treatment efficacy (probability that a worm is killed by a single round of treatment), x, the number of worms removed from compartment i at age a is binomially distributed ($w_i \sim \text{Binom}(P_i(a-1), x)$). The total number of worms killed across all compartments (z) is given by $z = \sum_{i=1}^{n} w_i$.

If either antibody response is stimulated by antigens from dying worms, this level is increased by z worms on the day of treatment, such that $G_j(a) = z + m_n$ when $S_j =$ dying adult worm antigen.

The decrease in infection rates after treatment is assumed to apply from the day after treatment, and to affect all individuals equally (in reality, it would take a few days for transmission rates to fall, but this is a short period in comparison to the 36 wk followed here, and this assumption is not expected to have a major effect). This is included as a reduction in the probability of infection per contact. The number of cercariae acquired on a "successful" contact, d, is multiplied by a factor φ, such that for any contacts made in the 36 wk after treatment, the number of new cercariae acquired in a single contact (t_q), is given by

$$t_q = \begin{cases} \varphi d & \text{if } s < 1/d, \text{ where } s \sim U(0,1) \\ 0 & \text{otherwise.} \end{cases} \quad \textbf{[S10]}$$

Estimating ϕ. A pilot mapping study was carried out to test whether exposure to *S. haematobium* infection correlated with distance lived from the nearest river water contact site, as was found in a previous study in Zanzibar (6). If this was the case, it was expected that infection intensities would be negatively correlated with this distance in young children who had not yet developed protective immunity against infection. After confirming this, the rates at which individuals in the study population (up to the age of 20 y) moved house were calculated, as a proxy for the rate at which they changed their contact rate (parameter ϕ).

Data sources. Age and parasitology data were collected as part of a cross-sectional study carried out in the Magaya schools and local community in the Murehwa district of Zimbabwe in September–November 2008 (7). As part of a pilot mapping study, a global positioning system (GPS) receiver was used to record the coordinates of active water contact sites used by residents of Magaya village, and the coordinates of the households of a number of study participants living in Magaya village. The straight-line distance between each participant's household and the nearest active water contact site was calculated using ArcGIS. When households were mapped, wherever possible information was obtained from adults in the household on the number of years that each study participant had lived in that household. Additional data were obtained from questionnaires given to a subset of the study participants as part of the main study, which included a question asking participants to list the number of previous villages that they had lived in.

Relationship between infection intensity and distance lived from nearest water contact site. A strong negative correlation was found between individual infection intensity and the distance between household and nearest active water contact site for 29 children in grades 0 or 1 of Magaya primary school, who were aged 4–8 years old (Fig. S1, Spearman's $\rho = -0.42$, $p = 0.023$). An even stronger negative correlation was found for the 19 children whose parents told us had lived there since they were born ($n = 19$) (Fig. S1, Spearman's $\rho = -0.59$, $p = 0.008$).

Rates of moving house. The rate of movement between households was calculated independently from two different datasets. Firstly, information gathered from adults interviewed during the household mapping studies was selected for the eldest child from each household mapped on how long they had lived in that household and whether they had lived there since birth. Only the eldest child was used to avoid potential biases from siblings moving to households at the same time. Data were available for individuals from 42 different households. The moving rate was calculated as the number of children who had moved to their current household since birth divided by the total length of time that all children

had lived in their current household. Twenty-one of the children had moved to their current household since birth, and a total of 367.3 y of residence in current household was reported across all 42 individuals, giving a moving rate of 0.057 per year.

The second method used to estimate moving rates came from questionnaire data for 283 individuals under the age of 20 y. The number of previous villages which individuals reported living in were added up for each person, and divided by the summed ages for all of these individuals. One hundred seventy-nine moves were reported altogether, and the total summed ages came to 3,447 y, giving a moving rate of 0.052 per year. Although this method will have missed within-village moves, interviews in the household survey suggested that the majority of local moves occurred between villages.

Both estimates of moving rate (ϕ) were very similar, and so a final value of 0.05 y^{-1} was used in the model.

Pattern-Oriented Modeling. Pattern-oriented modeling (POM) has been developed in ecology for agent (or individual)- based simulation models (8). In this approach, models are identified which can simultaneously reproduce multiple patterns observed in real systems at different levels or scales. This can guide the design of model structure and aid parameter estimation. In very different settings, POM has been used to discriminate between different possible model structures and to greatly narrow down potential parameter ranges and combinations (9–12). This approach allows both quantitative and qualitative patterns to be considered, and the use of multiple different patterns increases their ability to discriminate between different model structures and parameters. Additional details are given in our earlier paper, where POM was also used (3).

Model Criteria. Criteria were drawn up to test whether models could reproduce the required patterns of infection and antibody seen in field data. The following cross-sectional patterns in infection data were characterized and quantified: the peaked age intensity curve, reduced infection level in adults, the peak shift, aggregation of infection (by age) and infection prevalence (by age). For the antibody data, the following patterns were characterized: the antibody switch, the age at which the antibody switch occurs, and changes in antibody levels after treatment. Aggregation of antibody was assessed by age but was not included as a formal criterion since the range of standardized variances for the different antibody isotypes obtained from field data was too broad to be informative.

The data and methods used to draw up the peaked age intensity curve criterion and the reduced infection level in adults criterion have been previously described (3). Briefly, data on *S. haematobium* infection from six communities in Zimbabwe (7, 13, 14) were used to calculate mean infection levels in five age groups ($\leq$8-, 9–10-, 11–12-, 13–23-, and 24–34-year-olds), and age-specific infection levels from 15 additional populations were taken from the published literature (15–23). From all of these studies, the youngest and oldest age groups in which peak intensity was recorded were found to be 5–8 years old and 13–23 years old, respectively. Further analysis of the dataset with intensity peaking in 5–8-year-olds found that infection peaked in the upper end of this age group, and so the criteria was set to accept an infection peak occurring in any age group in between but not including 3–5-year-olds and 24–34-year-olds. All of the datasets that used arithmetic means (12 datasets) were used to identify the minimum and maximum levels of infection in adults as a percentage of the peak intensity ("reduced infection level in adults"). A range for this value of 5–26% was found, with some instability in the higher values depending upon the age groupings used, so a wider range of 0–40% was used as a conservative criterion. The peak shift, which has been demonstrated for infection curves for *S. mansoni* in Kenya (24) and *S. haematobium* in Zimbabwe (25) was included as a qualitative criterion. While the peak shift is a strong pattern across large numbers of populations, variability in field data means that it is not always seen between individual study sites, and so here it is assessed on the average values of peak age group and peak infection level over all repeat simulations for different values of the maximum infection rate.

Prevalence and aggregation of infection were calculated for the six Zimbabwean communities for the whole population and for two age groups (6–14- and 15–34-year-olds); only two age groups were used to give sufficiently large group sizes to give stable variance estimates. The two age groups were chosen to coincide with the age of the "switch" in antibody isotypes seen in two of these populations (13, 26). Infection aggregation was characterized by the standardized variance, calculated as $\sigma^2/\bar{x}^2$.

Fig. S2 shows the prevalence and standardized variance for each of the analyzed populations overall and by age group. Overall prevalence of infection (up to the age of 34 y) varied from 9.8–67.6%, and prevalence in the younger age group (0–14-year-olds) varied more widely from 9.6–76.6%. A slightly broader range of 5–80% was used for the infection prevalence criterion, applied separately to each of the two age groups. Standardized variance in infection in the whole population varied between 5.8 and 50.6, and between 4.2 and 59.3, and 4.0 and 29.0 in the 0–14-year-olds and 15–34-year-olds, respectively. Slightly wider ranges of 2–60 for each age group and the overall population were used for the aggregation criteria.

The data and methods used to draw up the antibody switch criteria have been previously described (3). Briefly, data for different antibody isotypes from two populations (13) were assessed for significant negative correlations (using a two-tailed Spearman's rank correlation coefficient) in pairwise comparisons, and for the five pairs of isotypes found that did display these negative correlations, it was found that these isotypes changed significantly with age in opposite directions (one of the pair increased with age and the other decreased, assessed using a Kruskal–Wallis test, with age as a categorical variable in the five age groups used to assess the infection intensity profiles). For the negative correlations that were significant at the 1% level, the correlation coefficient varied between -0.662 and -0.247. The criterion used to judge whether the models reproduced the antibody switch specified a Spearman's rank correlation coefficient of < -0.2. As described previously (3), for all of these antibody switches, the switch occurred at an older age than the age of peak infection intensity, and this was used as an additional criterion.

For the post-treatment antibody switch, the extent of the switch and the length of time over which the antibody responses remained switched were analyzed, using data from a subset of the Burma Valley population aged 6–15 years old for whom schistosome egg-antigen (SEA)-specific IgA and IgG1 were measured pre-treatment and 18, 24, 30 and 36 wk after praziquantel treatment (26). The data used is shown in Fig. S3. IgG1 showed a substantial increase after treatment, and IgA a very rapid drop. A conservative limit for identifying such a switch in model outputs (substantially exceeded in this dataset) was set as a doubling in the early (nonprotective) response, and a halving of the late (protective) response, seen at both 18 and 36 wk post-treatment.

The criteria are all listed and defined in Table 1. Apart from the peak shift, all other criteria were assessed for individual simulations. Initially it was planned to use formal criteria to test whether the models were able to reproduce observed aggregated distributions of antibody, but it was found that the range of standardized variances for the different antibody isotypes obtained from field data was too broad to be informative. Antibody aggregation and co-distributions were assessed visually for a subset of the models which passed all of the criteria for qualitative comparison with the field data.

1. Chan MS, Mutapi F, Woolhouse MEJ, Isham VS (2000) Stochastic simulation and the detection of immunity to schistosome infections. *Parasitology* 120:161–169.
2. de Vlas SJ (1996) Modelling human *Schistosoma mansoni* infection: The art of counting eggs in faeces. PhD thesis (Erasmus, Rotterdam, The Netherlands).
3. Mitchell KM, Mutapi F, Savill NJ, Woolhouse MEJ (2011) Explaining observed infection and antibody age-profiles in populations with urogenital schistosomiasis. *PLoS Comput Biol* 7:e1002237.
4. Lanzavecchia A, Sallusto F (2002) Progressive differentiation and selection of the fittest in the immune response. *Nat Rev Immunol* 2:982–987.
5. Gett AV, Sallusto F, Lanzavecchia A, Geginat J (2003) T cell fitness determined by signal strength. *Nat Immunol* 4:355–360.
6. Rudge JW, et al. (2008) Micro-epidemiology of urinary schistosomiasis in Zanzibar: Local risk factors associated with distribution of infections among schoolchildren and relevance for control. *Acta Trop* 105:45–54.
7. Mutapi F, et al. (2011) *Schistosoma haematobium* treatment in 1–5 year old children: Safety and efficacy of the antihelminthic drug praziquantel. *PLoS Negl Trop Dis* 5:e1143.
8. Grimm V et al. (2005) Pattern-oriented modeling of agent-based complex systems: Lessons from ecology. *Science* 310:987–991.
9. Janssen MA, Radtke NP, Lee A (2009) Pattern-oriented modeling of commons dilemma experiments. *Adapt Behav* 17:508–523.
10. Rossmanith E, Blaum N, Grimm V, Jeltsch F (2007) Pattern-oriented modelling for estimating unknown pre-breeding survival rates: The case of the lesser spotted woodpecker *(Picoides minor)*. *Biol Conserv* 135:555–564.
11. Swanack TM, Grant WE, Forstner MRJ (2009) Projecting population trends of endangered amphibian species in the face of uncertainty: A pattern-oriented approach. *Ecol Modell* 220:148–159.
12. Wiegand K, Saltz D, Ward D, Levin SA (2008) The role of size inequality in self-thinning: A pattern-oriented simulation model for arid savannas. *Ecol Modell* 210:431–445.
13. Mutapi F, Ndhlovu PD, Hagan P, Woolhouse MEJ (1997) A comparison of humoral responses to *Schistosoma haematobium* in areas with low and high levels of infection. *Parasite Immunol* 19:255–263.
14. Mutapi F et al. (2007) Cytokine responses to *Schistosoma haematobium* in a Zimbabwean population: Contrasting profiles for IFN-γ, IL-4, IL-5 and IL-10 with age. *BMC Infect Dis* 7:139.
15. Wilkins HA, Goll PH, de C Marshall TF, Moore PJ (1984) Dynamics of *Schistosoma haematobium* infection in a Gambian community. III. Acquisition and loss of infection. *Trans R Soc Trop Med Hyg* 78:227–232.
16. Bradley DJ, McCullough FS (1973) Egg output stability and the epidemiology of *Schistosoma haematobium*. II. An analysis of the epidemiology of endemic *S. haematobium*. *Trans R Soc Trop Med Hyg* 67:491–500.
17. Clarke, VD (1966) The influence of acquired resistance in the epidemiology of bilharziasis. *Cent Afr J Med* 12:1–30.
18. Useh MF, Ejezie GC (1999) Modification of behaviour and attitude in the control of schistosomiasis. 1. Observations on water-contact patterns and perception of infection. *Ann Trop Med Parasitol* 93:711–720.
19. Wilkins HA, Blumenthal UJ, Hagan P, Hayes RJ, Tulloch S (1987) Resistance to reinfection after treatment of urinary schistosomiasis. *Trans R Soc Trop Med Hyg* 81:29–35.
20. Agnew A, et al. (1996) Age-dependent reduction of schistosome fecundity in *Schistosoma haematobium* but not *Schistosoma mansoni* infections in humans. *Am J Trop Med Hyg* 55:338–343.
21. Chandiwana SK, Taylor P, Clarke, VD (1988) Prevalence and intensity of schistosomiasis in two rural areas in Zimbabwe and their relationship to village location and snail infection rates. *Ann Trop Med Parasitol* 82:163–173.
22. Ndhlovu P, et al. (1996) Age-related antibody profiles in *Schistosoma haematobium* infections in a rural community in Zimbabwe. *Parasite Immunol* 18:181–191.
23. King C, Muchiri E, Ouma JH (1992) Age-targeted chemotherapy for control of urinary schistosomiasis in endemic populations. *Mem Inst Oswaldo Cruz* 87:203–210.
24. Fulford AJC, Butterworth AE, Sturrock RF, Ouma JH (1992) On the use of age-intensity data to detect immunity to parasitic infections, with special reference to *Schistosoma mansoni* in Kenya. *Parasitology* 105:219–227.
25. Woolhouse MEJ, Taylor P, Matanhire D, Chandiwana SK (1991) Acquired immunity and epidemiology of *Schistosoma haematobium*. *Nature* 351:757–759.
26. Mutapi F, et al. (1998) Chemotherapy accelerates the development of acquired immune responses to *Schistosoma haematobium* infection. *J Infect Dis* 178:289–293.

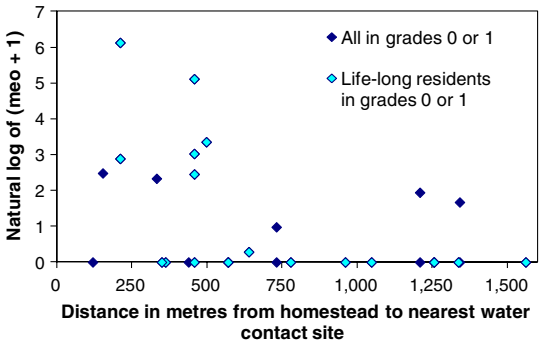

Fig. S1. Relationship between infection intensity (natural log of meo (mean egg output) + 1, where egg counts come from two or three 10-mL urine samples collected on consecutive days), and distance lived from water contact site (straight line distance in meters between household and nearest active water contact site on a river) for children in grades 0 or 1 at Magaya primary school. Data shown for all of the children in this group ($n = 29$, dark blue diamonds) and highlighted for those who were life-long residents at their current household ($n = 19$, light blue diamonds).

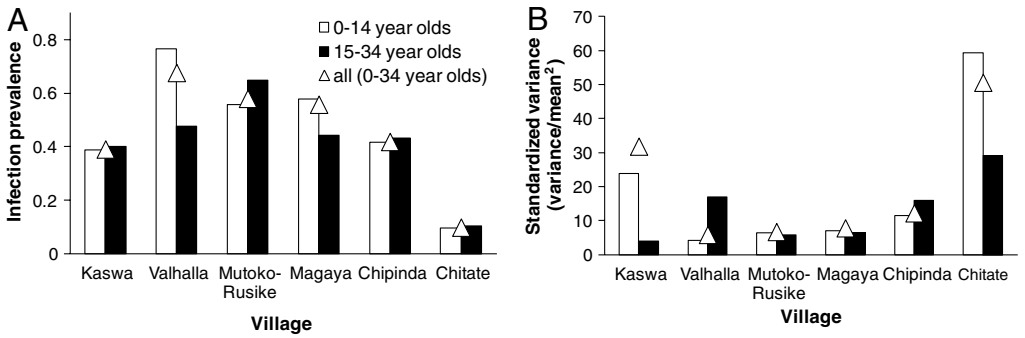

Fig. S2. (*A*) Prevalence and (*B*) standardized variance for infection levels for each of the six populations by two age groups and all together.

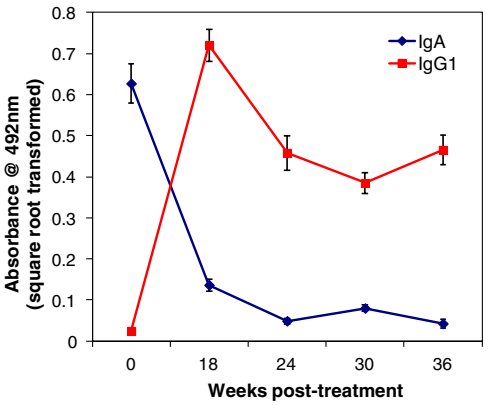

Fig. S3. Changes in antibody levels after treatment. Levels of SEA IgA and IgG1 in a cohort of 6–15-year-olds from Valhalla and Kaswa before treatment and 18, 24, 30, and 36 wk post-treatment with praziquantel. Sample sizes were 73, 66, 61, 52, and 48 at 0, 18, 24, 30, and 36 wk, respectively. Data previously published in ref. 26.

Table S1. Parameters used in the models, with ranges explored in the baseline analysis, additional values used in the sensitivity analysis, units and sources from the literature where relevant

Parameter*	Meaning	Values used in baseline analysis	Values used in sensitivity analysis	Units†	Source/rationale
Λ_{pmax}	Mean population maximum contact rate	12.5,25,50,100,200		worms year^{-1} person^{-1}	Ref. 1
a_c	Age above which contact rates stay constant	7.8		years of age	Fit to data from Ref. 1
ϕ	Probability of resampling individual maximum contact rate	0.05	0,0.5	year^{-1}	Supplementary Material, 'Estimating ϕ'
k_1	Shape parameter for the distribution of individual maximum contact rates	0.5	0.4, ∞	no units	Ref. 2
d	Number of cercariae acquired in a contact with probability $1/d$	1	10,100	contact^{-1}	Varied to give different degrees of cercarial aggregation
n	Number of worm compartments in model	9		compartments	Approx. Gaussian distributed worm survival
$1/\mu$	Natural mean worm life span	3,6.5,10		years	Refs. 3, 4
ε	Eggs output per worm per 10 mL urine	1	0.1,10	eggs worm^{-1} d^{-1} 10 mL urine^{-1}	Ref. 5
k_E	Shape parameter for egg output per worm	1	∞	no units	Ref. 6
κ_j	Rate of production of plasma cells	1		cells year^{-1} unit antigen^{-1}	Variation accounted for in varying immune strength
γ_j	Rate of loss of plasma cells	0.008,0.08,0.8,8,80		cells year^{-1} cell^{-1}	Refs. 7, 8
θ	Strength of protection against reinfection	0.00025,0.001,0.004, 0.016,0.064,0.256,1.024		cell^{-1}	Broad exploratory range
η	Strength of anti-fecundity response	0.00025,0.001,0.004, 0.016,0.064,0.256,1.024		cell^{-1}	Broad exploratory range
ρ	Strength of cross-regulation	0.001,0.1,1		unit antigen^{-1}	Set to give significant effect on immune development
β	Rate of production of "cumulative" response	1		arbitrary units year^{-1} unit antigen^{-1}	Arbitrary constant
T	Threshold for cumulative antigen exposure	25,250,2500		antigen units	Set to give significant effect on age-intensity curve
x	Treatment efficacy	0.8,0.9,1.0		proportion of worms killed	Ref. 9

Parameter*	Meaning	Values used in baseline analysis	Values used in sensitivity analysis	Units†	Source/rationale
φ	Post-treatment reduction in infection probability	0,0.5,1		proportion	Explored across full possible range

*Subscript j refers to values for the two different antibody responses ($j = 1, 2$).

†'cell' = unit of the plasma B cell population; antigen units = number of cercariae/live worms/dying worms/eggs as appropriate.

1 Chan MS, Mutapi F, Woolhouse MEJ, Isham VS (2000) Stochastic simulation and the detection of immunity to schistosome infections. *Parasitology* 120:161–169.
2 Woolhouse MEJ, Etard JF, Dietz K, Ndhlovu PD, Chandiwana SK (1998) Heterogeneities in schistosome transmission dynamics and control. *Parasitology* 117:475–482.
3 Fulford AJC, Butterworth AE, Ouma JH, Sturrock RF (1995) A statistical approach to schistosome population-dynamics and estimation of the life-span of *Schistosoma mansoni* in man. *Parasitology* 110:307–316.
4 Wilkins HA, Goll PH, de C Marshall TF, Moore PJ (1984) Dynamics of *Schistosoma haematobium* infection in a Gambian community. III. Acquisition and loss of infection. *Trans R Soc Trop Med Hyg* 78:227–232.
5 Hairston NG (1965) On the mathematical analysis of schistosome populations. *Bull World Health Organ* 33:45–62.
6 de Vlas SJ (1996) Modelling human *Schistosoma mansoni* infection: The art of counting eggs in faeces. PhD thesis (Erasmus, Rotterdam, The Netherlands).
7 Ochsenbein AF, et al. (2000) Protective long-term antibody memory by antigen-driven and T help-dependent differentiation of long-lived memory B cells to short-lived plasma cells independent of secondary lymphoid organs. *Proc Natl Acad Sci USA* 97:13263–13268.
8 Amanna IJ, Carlson NE, Slifka MK (2007) Duration of humoral immunity to common viral and vaccine antigens. *N Engl J Med* 357:1903–1915.
9 Danso-Appiah A, Utzinger J, Liu J, Olliaro P (2008) Drugs for treating urinary schistosomiasis. *Cochrane Database Syst Rev* 3:CD000053.